American Journal of Computational Mathematics, 2025, 15(2), 191-208
https://www.scirp.org/journal/ajcm
ISSN Online: 2161-1211
ISSN Print: 2161-1203

Numerical Investigation of Free Convection of MHD-Nanofluid in a Square Cavity with a Heated Cone

Saika Mahjabin[1], Md. Abdul Alim[2]

[1]Department of Mathematics, National University, Gazipur, Bangladesh
[2]Department of Mathematics, Bangladesh University of Engineering & Technology, Dhaka, Bangladesh
Email: mahjabinsaika.bd@gmail.com, maalim@math.buet.ac.bd

How to cite this paper: Mahjabin, S. and Alim, M.A. (2025) Numerical Investigation of Free Convection of MHD-Nanofluid in a Square Cavity with a Heated Cone. *American Journal of Computational Mathematics*, **15**, 191-208.
https://doi.org/10.4236/ajcm.2025.152010

Received: March 28, 2025
Accepted: June 27, 2025
Published: June 30, 2025

Abstract

Free convection of Magnetohydrodynamic (MHD) fluid, seeded with nanoparticles, in a square cavity with a heated cone inside, has been investigated numerically in this work. The mathematical model is developed by combining the mass, momentum and energy equations. The system of equations is solved by finite element method. Calculations are performed for different values of the dimensionless parameters: Prandtl number (*Pr*), Rayleigh number (*Ra*), Hartmann number (*Ha*) and the volume fraction of the nanoparticle (φ). The results are illustrated with streamlines, velocity profiles, isotherms, local and average Nusselt number (*Nu*), and heat flux. It is found that, the volume fraction of nanoparticle (φ) is the most important parameter affecting the entire convection process. Adding nanoparticles significantly slows down the fluid velocity, but enhances the heat transfer. The effect of varying φ, surpasses the effects of all other governing parameters with regards to heat transfer.

Keywords

Free Convection, MHD, Nano Fluid, Hartmann Number, Square Cavity, Heated Cone

1. Introduction

Nano materials are very interesting to the scientific community due to their unusual properties, which arises out of their sizes. Much research is done to invent new materials of nano scale, and studying their properties and exploring suitable practical applications. Consequently, many claims are made regarding the benefits of using them in a wide range of practical applications. This paper, however, focused on the thermo-fluidic behavior of nano fluid. Heat exchangers are widely used, from very small scale such as for cooling computer processors, to the mega-scale such as nuclear power plants. Thus, designing efficient and robust heat exchangers have been a perpetual challenge. Nanoparticles with their unique properties have opened up new avenues to pursue the quest for the "ideal" heat exchanger. Moreover, fluid motion and heat transfer around a cone has many scientific and engineering applications. Conical shapes are found in flow and pressure control valves, high speed aircrafts and projectiles, deep sea probes and so on. According to NASA, the air around high-speed flying objects becomes ionized and shows MHD behavior [1]. Thus, combining conical shape and MHD nano fluid makes the study important. This paper presents the results from the research carried out by Mahjabin [2]. That work was done in two sections. The first section dealt with MHD fluid without the nano particles, and the results were published previously [3] [4]. This paper is focused on the second section, and will systematically present the results found for different concentration of nano particles, and intensities of the magnetic field, and point out the practical implications where applicable.

2. Literature Review

Nanomaterials have opened a new frontier for research due to their profound influence on the properties of matter. Fluids seeded with nanomaterials are found to influence thermophysical properties and significantly affect heat transfer. Consequently, this attracted many researchers. Most of the researches are carried out by numerical techniques, as it is extremely difficult to conduct experimentally. Again, most of the investigations involved various types of enclosures and thermal boundaries. The results are reported in terms of dimensionless parameters, the most common being the Raleigh number (*Ra*), Hartmann number (*Ha*), Nusselt number (*Nu*), Grashoff number (*Gr*), and Prandtl number (*Pr*). A brief literature review, in chronological order, should illustrate this.

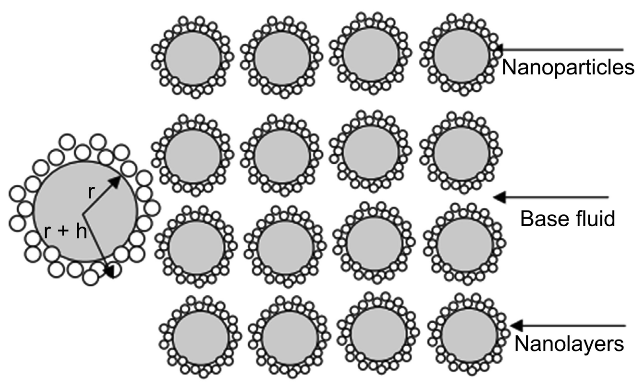

Figure 1. Structures of nanofluids [7].

Chamkha *et al.* provided one of the early reviews on the state and challenges of nanofluid research [5]. They reviewed many works published at that time, summarized them, and provided some basic equations and methodologies, which are widely adopted in many researches later on. Choi clearly demonstrated that the thermal conductivity of fluids can be enhanced by nanoparticles [6]. Later, Yu and Choi attempted to explain heat transfer by proposing the structure of nanofluids, as shown in **Figure 1** [7].

Khanafer *et al.* showed that, in a two-dimensional enclosure, the heat transfer rate increases substantially with the increase in φ for all values of *Gr* [8]. Jou and Tzeng, applying Khanafer's model, noted that increasing *Gr* and φ enhances the average heat transfer coefficient considerably [9]. Tiwari and Das developed a model to analyze the behaviors of nanofluids inside a lid-driven square cavity [10]. They found that the fluid flow and heat transfer in the cavity were affected by the Richardson number and the direction of moving walls. Saidur *et al.* discussed a wide range of practical applications of nanofluids such as engine cooling, solar water heating, cooling of electronics, transformer oil, improving diesel generator efficiency, heat exchangers, chillers, domestic refrigerator-freezers, nuclear reactors, etc. [11]. They stated that heat transfer can be enhanced by nanofluids. They also stated that the exact mechanism of enhanced heat transfer for nanofluids was still unclear. They also mentioned some major obstacles to the practical applications of nanofluids such as stability and production cost. Qi *et al.* simulated convection in nanofluids with a two-phase Lattice Boltzmann model [12]. They noted the rapid increase in *Nu* with φ and *Ra*. Sheremet *et al.* utilized the Tiwari and Das nanofluid model in a differentially heated porous square cavity [13]. It showed that *Nu* was an increasing function of *Ra*. Lattice Boltzmann model was also applied by other researchers like Nemati *et al.*, Ahmed and Eslamian, and so forth [14] [15]. Mokaddes *et al.* also investigated grooved enclosures considering Brownian motion and showed that the heat transfer increases with *Ra* and φ, but decreases with increasing *Ha*. Moreover, the heat transfer rate accelerates significantly in the presence of square grooves [16]. In a subsequent work, Mokaddes *et al.* considered entropy generation as well [17]. They showed that the average *Nu* and entropy generation increase with rising *Ra* and φ, decreasing with increasing *Ha*. They also attempted to find the combination of governing parameters to maximize heat transfer and minimize entropy generation. Chamkha *et al.* studied the case of a rotating cone in 2D/3D mixed convection [18]. They used carbon nanotube (CNT)-water nanofluid in a double lid-driven porous trapezoidal cavity. They showed that the average *Nu* is higher for the 2D case. The gap between the *Nu* values for the 2D and 3D cases increases with rotational speed. Also, *Ha* reduced the effective convection, but *Nu* increased due to the highly conductive CNT particles. Alomari *et al.* studied a hybrid nanofluid (MgO-Ag/water) in a trapezoidal cavity, subjected to sinusoidal heating from the bottom wall [19]. They reported that the strength of the stream functions increases with *Ra* and φ, while increasing *Ha* reduces the circulation of the flow. Heat transfer, as indicated by *Nu,* increases with *Ra* and φ while it decreases with *Ha*. Mondal *et al.* used an Al2O3-water MHD fluid and considered the entropy generation along with convection [20]. They observed a decreasing trend of average *Nu* and Sherwood numbers with *Ha* and the volume fraction of the nanoparticles (φ). Sannad *et al.* used different diameters of nanoparticles and concluded that the concentration in the base fluid plays the most important role in the heat transfer characteristics [21]. Abdelhameed reported that the magnetic field and porosity have a strong influence on velocity, entropy generation, and Bejan number. Moreover, the entropy generation can decrease with greater porosity [22]. Similarly, many other works may be cited, however, the following general observations apply:

1) In addition to the *Ra* and *Ha*, the volume fraction of the nanoparticles, φ, affects the heat transfer and fluid flow in varying degrees. Increasing *Ra* increased circulation and heat transfer while increasing *Ha* had the opposite effect.

2) Boundary conditions of the enclosures have a significant influence on heat transfer and fluid flow.

3) The properties and concentration of the nanoparticle play the most important role regarding heat transfer and flow behavior.

The novelty of this work lies in the presence of the heated cone, and applying nanoparticles and magnetic field simultaneously. It opened an opportunity to study the relative weights of these two extraneous parameters, namely the magnetic field's intensity (*Ha*), and the volume fraction of the nano particle (φ), on the convection process in an MHD fluid.

3. Physical Model

Figure 2 shows a schematic diagram of the model. The cavity is filled with an MHD fluid, in addition there is nano particles suspended in it. The left and right vertical walls of the cavity are thermally insulated, while the bottom and top walls are kept at different high (T_h) and low (T_c) temperatures respectively. The heated cone is kept at vertical position only. A magnetic field of uniform intensity B_0 is applied, perpendicular to the direction of flow. The gravitational force *g*, acts vertically downward.

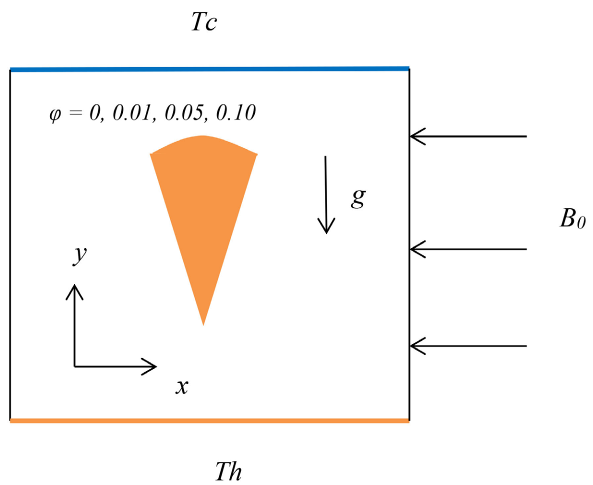

Figure 2. Schematic diagram of the model.

4. Mathematical Formulation

The steps for mathematical formulation are briefly outlined next.

4.1. Governing Equation in Dimensional Form

The base flid is assumed Newtonian and incompressible. The fluid flow is laminar in the laminar regime, set in motion by free convection. The fluid properties are assumed constant. The density variation is treated according to Boussinesq approximation, while the viscous dissipation effects are neglected. The viscous incompressible flow and the temperature distribution inside the cavity are described by the Navier-Stokes and the energy equations, respectively. The governing equations of the present problem are as follows:

Conservation of mass:

$$\frac{\partial u}{\partial x}+\frac{\partial v}{\partial y}=0 \tag{1}$$

Conservation of momentum:

$$u\frac{\partial u}{\partial x}+v\frac{\partial u}{\partial y}=-\frac{1}{\rho_{nf}}\frac{\partial p}{\partial x}+\frac{\mu_{nf}}{\rho_{nf}}\left(\frac{\partial^2 u}{\partial x^2}+\frac{\partial^2 u}{\partial y^2}\right) \tag{2}$$

$$\begin{aligned} u\frac{\partial v}{\partial x}+v\frac{\partial v}{\partial y}=&-\frac{1}{\rho_{nf}}\frac{\partial p}{\partial y}+\frac{\mu_{nf}}{\rho_{nf}}\left(\frac{\partial^2 v}{\partial x^2}+\frac{\partial^2 v}{\partial y^2}\right)\\ &+\frac{1}{\rho_{nf}}\left[g\beta_{nf}\rho_{nf}\left(T-T_c\right)\right]-\frac{1}{\rho_{nf}}\left[\sigma_{nf}B_0^2 v\right] \end{aligned} \tag{3}$$

Conservation of Energy:

$$u\frac{\partial T}{\partial x}+v\frac{\partial T}{\partial y}=\alpha_{nf}\left(\frac{\partial^2 T}{\partial x^2}+\frac{\partial^2 T}{\partial y^2}\right) \tag{4}$$

Properties of the nanofluid are combinations of the properties of the base fluid, denoted by the subscript "*f*", and those of the nanoparticle, denoted by the subscript "*s*". These properties are defined as follows:

Effective density

$$\rho_{nf}=(1-\phi)\rho_f+\phi\rho_s$$

where φ is the solid volume fraction of nanoparticles.

Heat capacitance

$$\left(\rho C_p\right)_{nf}=(1-\phi)\left(\rho C_p\right)_f+\phi\left(\rho C_p\right)_s$$

Thermal expansion coefficient

$$\beta_{nf}=(1-\phi)\beta_f+\phi\beta_s$$

Thermal diffusivity

$$\alpha_{nf}=k_{nf}\Big/\left(\rho C_p\right)_{nf}$$

Electrical conductivity

$$\sigma_{nf} = \sigma_f \left[1 + \frac{3\varphi\left(\frac{\sigma_s}{\sigma_f} - 1\right)}{\left\{\left(\frac{\sigma_s}{\sigma_f}\right) + 2\right\} - \left\{\left(\frac{\sigma_s}{\sigma_f}\right) - 1\right\}\varphi} \right] \quad [23]$$

Thermal conductivity

$$k_{nf} = k_f \left[\frac{(k_s + 2k_f) - 2\varphi(k_f - k_s)}{(k_s + 2k_f) + \varphi(k_f - k_s)} \right] \quad [24]$$

Viscosity

$$\mu_{nf} = \mu_f \left(1 + 39.11\varphi + 533.9\varphi^2\right) \quad [25]$$

4.2. Boundary Conditions

At the bottom wall:

$$u(x,0) = 0, \quad v(x,0) = 0, \quad T = T_h, \quad \forall\, y = 0, \quad 0 \le x \le L$$

At the left wall:

$$u(0,y) = 0, \quad v(0,y) = 0, \quad \partial T/\partial x = 0, \quad \forall\, x = 0, \quad 0 \le y \le L$$

At the right wall:

$$u(0,y) = 0, \quad v(0,y) = 0, \quad \partial T/\partial x = 0, \quad \forall\, x = L, \quad 0 \le y \le L$$

At the top wall:

$$u(x,L) = 0, \quad v(x,L) = 0, \quad T = T_c, \quad \forall\, y = L, \ 0 \le x \le L$$

4.3. Dimensional Analysis

To obtain non-dimensional governing equations, we incorporate the following dimensionless dependent and independent variables:

$$X = \frac{x}{L}, \ Y = \frac{y}{L}, \ U = \frac{uL}{\alpha_f}, \ V = \frac{vL}{\alpha_f}, \ P = \frac{pL^2}{\rho_{nf}\alpha_f^2} \ \text{ and } \ \theta = \frac{T - T_c}{T_h - T_c}$$

where X and Y are the coordinates varying along horizontal and vertical directions, respectively, U and V are the velocity components in the X and Y directions, respectively, θ is the dimensionless temperature, P is the dimensionless pressure, and α is the thermal diffusivity of the fluid.

After applying the above dimensionless variable, Equations (1)-(4) are transformed into dimensionless form as the following:

$$\frac{\partial U}{\partial X} + \frac{\partial V}{\partial Y} = 0 \quad (5)$$

$$U\frac{\partial U}{\partial X} + V\frac{\partial U}{\partial Y} = -\frac{\partial P}{\partial X} + \frac{\nu_{nf}}{\alpha_f}\left(\frac{\partial^2 U}{\partial X^2} + \frac{\partial^2 U}{\partial Y^2}\right) \quad (6)$$

$$U\frac{\partial V}{\partial X} + V\frac{\partial V}{\partial Y} = -\frac{\partial P}{\partial Y} + \frac{\nu_{nf}}{\alpha_f}\left(\frac{\partial^2 V}{\partial X^2} + \frac{\partial^2 V}{\partial Y^2}\right) + \left(\frac{\beta_{nf}}{\beta_f}\right) Ra Pr \theta - \left(\frac{\rho_f}{\rho_{nf}}\right)\left(\frac{\sigma_{nf}}{\sigma_f}\right) Ha^2 Pr V \quad (7)$$

$$U\frac{\partial\theta}{\partial X}+V\frac{\partial\theta}{\partial Y}=\frac{\alpha_{nf}}{\alpha_f}\left(\frac{\partial^2\theta}{\partial X^2}+\frac{\partial^2\theta}{\partial Y^2}\right) \tag{8}$$

Here the dimensionless parameters are defined as follows:

Prandtl number, $Pr=\frac{\nu}{\alpha}$ (ratio of viscous to thermal diffusion rates, which indicates the ratio or dominance of heat transfer mode-convection over conduction)

Hartmann number, $Ha=B_0L\sqrt{\frac{\sigma}{\mu}}$ (ratio of electromagnetic force to the viscous force)

Grashof number, $Gr=\frac{g\beta L^3\left(T_h-T_c\right)}{\nu^2}$ (ratio of the buoyancy to viscous force)

Rayleigh number, $Ra=\frac{g\beta L^3\left(T_h-T_c\right)Pr}{\nu^2}$ (product of Gr and Pr. It also indicates the ratio or dominance of heat transfer mode-convection over conduction, but incorporates the buoyancy force).

4.4. Dimensionless Boundary Conditions

The dimensionless boundary conditions become:

$U=V=0, \theta=1$ at bottom wall and heated conical body (at higher constant temperature)

$U=V=0, \theta=0$ at top wall (at lower constant temperature)

$U=V=0, \frac{\partial\theta}{\partial N}=0$ at side walls (thermally insulated)

$P=0$ Fluid pressure at the inside and on the walls of the cavity

where X and Y are dimensionless coordinates varying along horizontal and vertical directions, respectively; U and V are dimensionless velocity components in X and Y directions, respectively; θ is the dimensionless temperature.

5. Numerical Analysis

The above system of equations is solved along with the boundary conditions shown above, by finite element method. This technique is described by various researchers such as Dechaumphai [26], Reddy [27], Taylor and Hood [28]. In this method, the solution domain is discretized into finite element mesh. Then the nonlinear governing equations are transferred into a system of integral equations by applying the Galerkin weighted residual method. Gauss quadrature method is used to perform the integration involved in each term of these equations. The nonlinear algebraic equations thus obtained are modified by imposing boundary conditions. Then Newton's method is used to transform these modified equations into linear algebraic equations, and then these linear equations are solved by applying the triangular factorization method.

5.1. Grid Generation

The model is subdivided into many smaller discrete elements, and the set of equations are solved for each element. The mesh structure of finite elements for the present physical model displays in Figure 3.

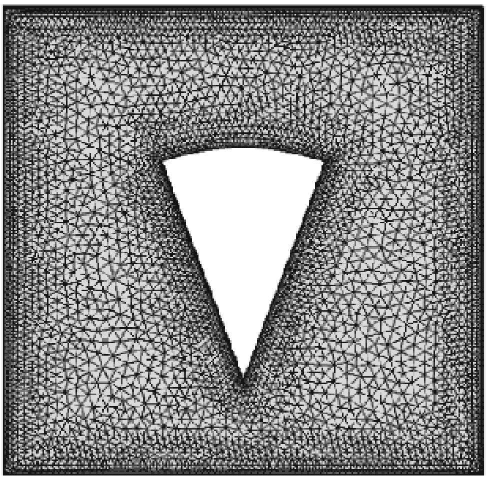

Figure 3. Mesh with 8039 elements.

5.2. Grid Refinement Check

Grid independence test was performed with different number of elements and the average Nusselt number was assumed to be the test variable. The results are shown in Table 1 and Figure 4.

Table 1. Grid sensitivity on Average Nusselt Number (Nu) by number of elements.

Number of Elements	Average *Nu*
670	0.14405
1218	0.14671
1794	0.14781
2663	0.14865
8039	0.14977
21,974	0.15013

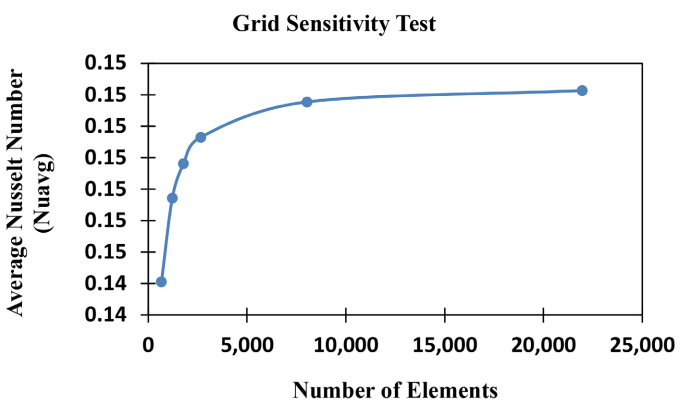

Figure 4. Grid sensitivity test ($Ha = 0$, $Ra = 10^5$).

It is seen that after about 8000 elements, further refinement does not have any appreciable impact on the average Nusselt number. Therefore, grid independence is attained around 8000. The present model used 8039 elements for the computations. Table 2 shows the thermo physical properties of the base fluid and the nano particle.

Table 2. Properties of the base fluid and the nano particle.

Physical property	Symbol (Unit)	Base Fluid	Nano Particle
Specific heat	C_p (J/kg-K)	14,179	540
Density	ρ (kg/m^3)	997.1	6500
Thermal conductivity	k (W/m-K)	0.613	18
Thermal expansion	β (1/K)	2.1×10^{-4}	0.085×10^{-4}
Electrical Conductivity	σ $(\Omega\cdot\text{m})^{-1}$	0.05	10^{-10}

6. Results and Discussions

The calculations are performed for a fixed Prandtl number $Pr = 6.2$. The Rayleigh numbers were $Ra = 1 \times 10^3$, 1×10^4, 1×10^5; the Hartmann numbers $Ha = 0$, 20, 40; and the volume fraction of nanoparticle $\varphi = 0$, 0.01, 0.05, and 0.10. The results were examined with streamlines, velocity profiles, isotherms, heat fluxes, average velocities, and average temperatures. Several observations were made from the results which are discussed next.

6.1. Fluid Flow Behavior (Streamlines and Velocities)

Figure 5 shows the effect of Ra on the streamlines with no nanoparticles ($\varphi = 0$) and no magnetic field ($Ha = 0$), as a baseline case. The streamlines represent the fluid flow pathways, while the colors represent the velocity. The velocity magnitude is indicated by the color legend shown at the right side of each figure.

At $Ra = 10^3$, two vortices are seen on both side of the cone. The velocity varies from 0.05 to 0.5. At $Ra = 10^4$, four additional major and two minor vortices appear, and the velocities increase by an order of magnitude. Further increase of Ra to 10^5, total number of vortices remains the same but their shapes changed. Velocity also increased noticeably. However, the flow patterns remain symmetric around the cone for all cases.

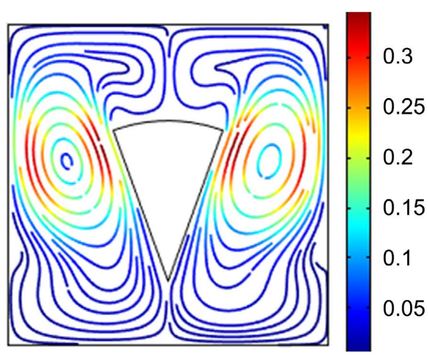

$Ra = 10^3$

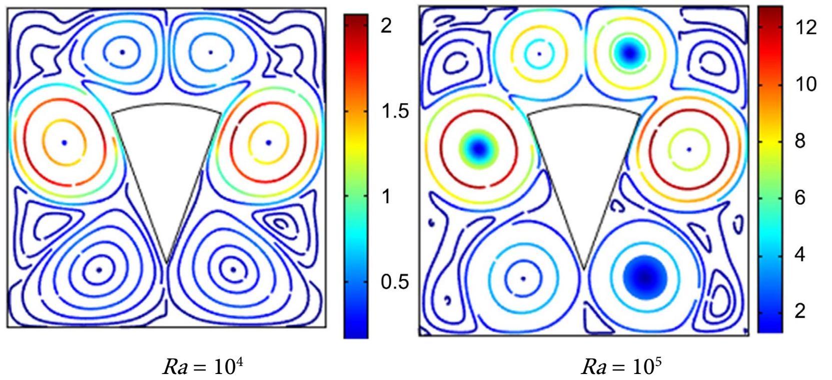

Figure 5. Streamlines for different *Ra*, $\varphi = 0$, $Ha = 0$.

Next, *Ra* is kept constant at 10^4, and the values of φ and *Ha* are increased. The reason for keeping *Ra* fixed at a high value is that, the effects of *Ha* become more pronounced at higher *Ra*'s, providing better understanding of the phenomenon being studied. The results are shown in **Figure 6**.

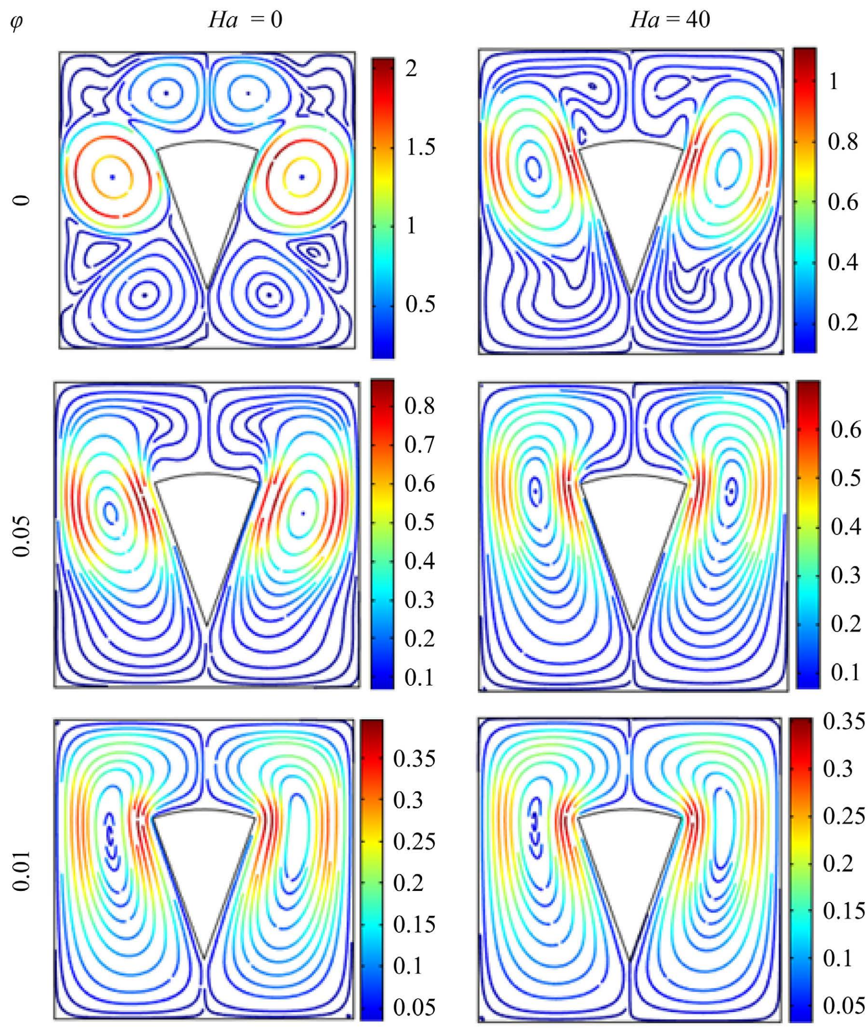

Figure 6. Streamlines for different *Ha* and φ, $Ra = 10^4$.

It is seen that with increasing φ, the additional vortices disappear, and the velocities reduce significantly. However, for a given φ, increasing *Ha* does not have much effect. With increasing φ, the effect of *Ha* becomes less and less noticeable. It implies that the nano-particles have a more dominating effect over the magnetic field to influence the fluid movement. The physical explanation to this behavior is that, adding nano particles makes the nano-fluid heavier, thus slowing down the motion. This dominated over magnetic field because the nano particles considered in this study has very low electrical conductivity and magnetic susceptibility.

6.2. Heat Transfer Behavior (Isotherms and Heat Flux)

Isotherms: Figure 7 show the effect of *Ra* on temperature distribution in the form of isotherms, with $\varphi = 0$, and $Ha = 0$. The labels next to the curves show the values of θ, the dimensionless temperature whose value range is from 0 to 1. The coloring also indicate temperature gradually changing from hotter to cooler (from red to green).

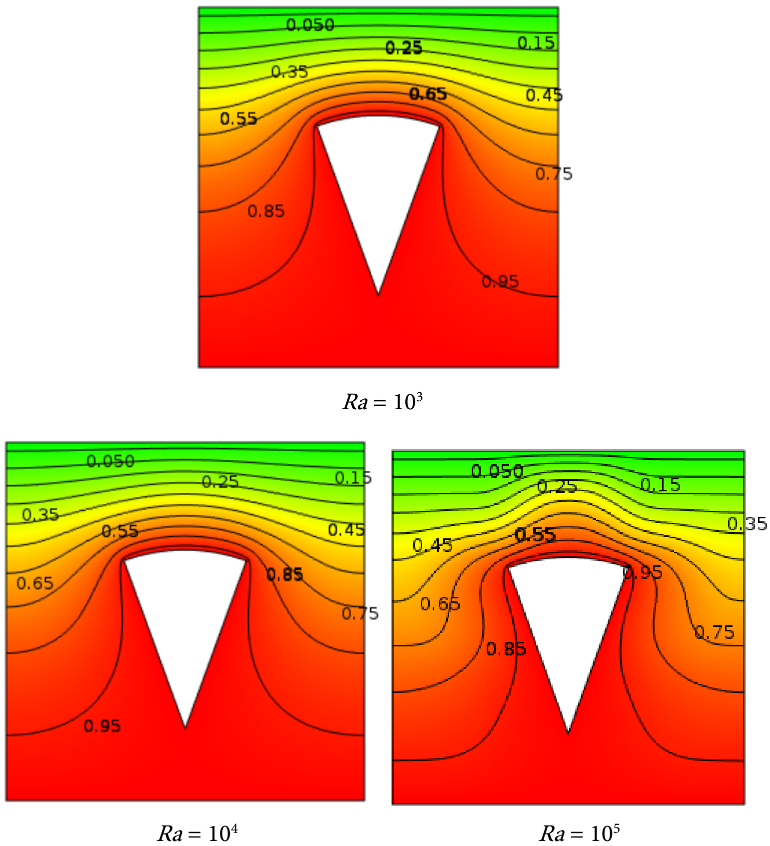

Figure 7. Isotherms for different *Ra*, $\varphi = 0$, $Ha = 0$.

It is noted that the distortion of the isotherms becomes more and more prominent with increasing *Ra*. The isotherm corresponding to 0.95 moved closer to the bottom wall with increasing *Ra*, indicating that the larger portion of the cavity is cooler.

Next, Ra is kept constant at 10^5, and the values of φ and Ha are increased. The reason for doing this is mentioned in the previous section. The results are shown in **Figure 8**. It is noted that, the nano-particles have a greater influence on the temperature distribution as well, compared to that of the magnetic field. Similar to the influence on fluid movement as seen in the previous section (**Figure 6**).

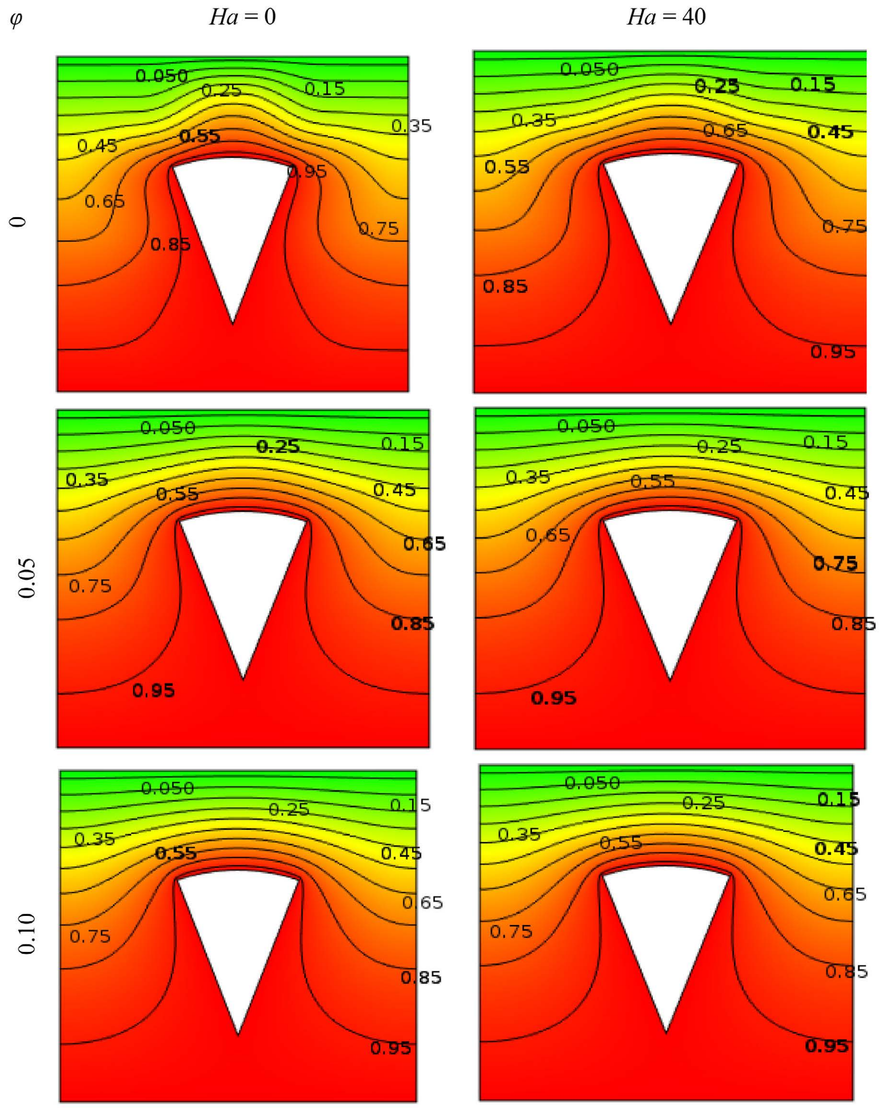

Figure 8. Temperature distribution for different Ha and φ, $Ra = 10^5$.

Heat flux: It is seen that in the previous figures that, adding more nanoparticle retarded flow. Increasing Hartmann number also retarded flow. Adding more nanoparticle also affected temperature distribution by making the isotherms smoother. Increasing Hartmann number also had similar effect but to a lesser degree. However, these observations are not sufficient to say conclusively whether heat transfer was enhanced or not. Therefore, Heat Flux was calculated for different values of Ra, Ha, and φ. The results are presented next in **Figure 9**.

Figure 9(a) shows the case of base fluid only, with no nano particles added. It is seen that the effect of *Ha* is quite noticeable at higher values of *Ra*. It also shows that, increasing *Ha* decreased the heat flux. Figures 9(b)-(d) are the cases with increasing concentration of nano particles. It is noted that while heat flux increased with *Ra*, the difference in heat flux due to different values of *Ha* almost vanished. In other words, the nano-particles just overwhelmed the heat transfer process, making the Magnetic field almost irrelevant.

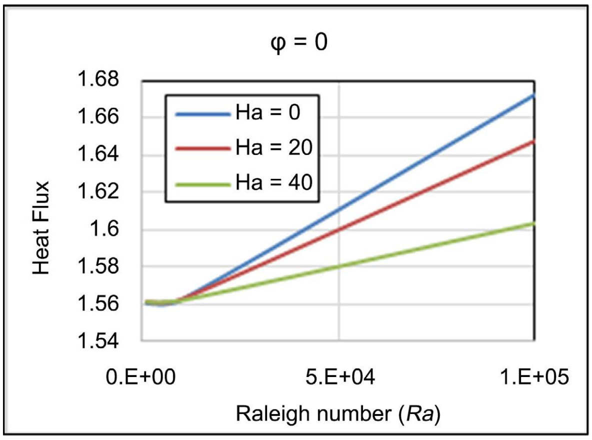

(a)

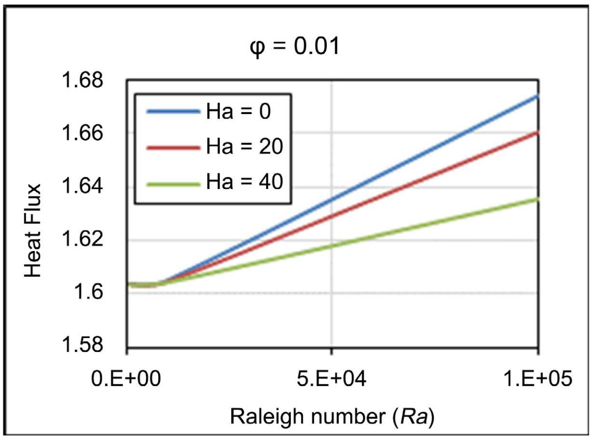

(b)

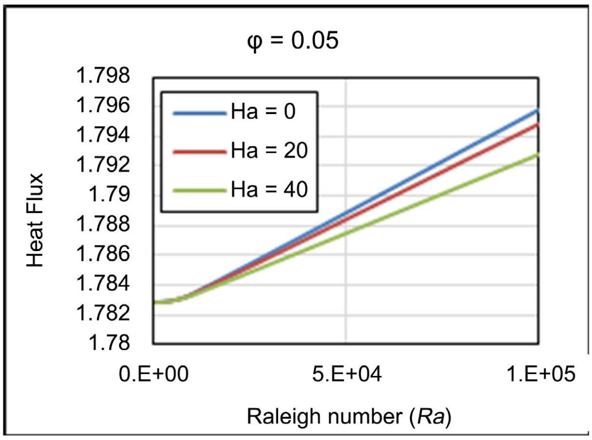

(c)

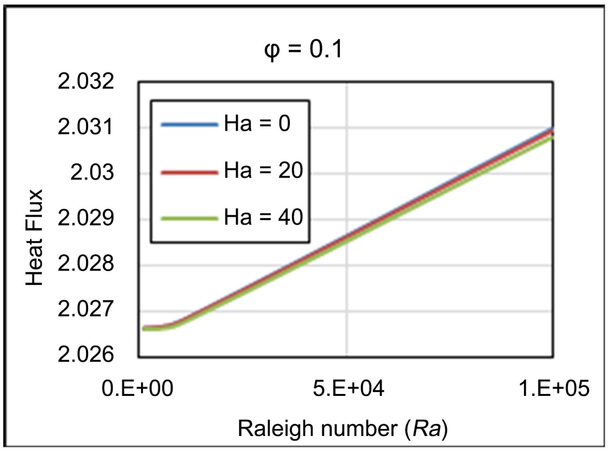

(d)

Figure 9. Effect of *Ha* on heat flux as a function of *Ra* for different values of *φ*.

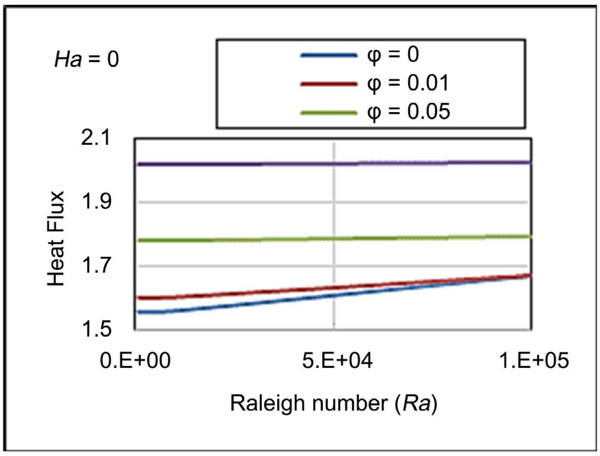

(a)

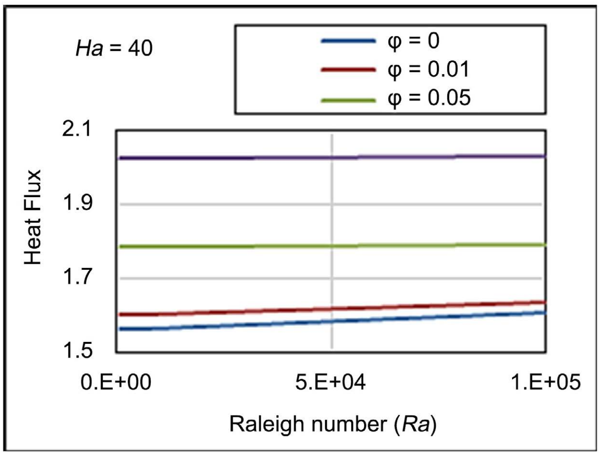

(b)

Figure 10. Effect of *φ* on heat flux as a function of *Ra* for different values of *Ha*.

Figure 10(a) compares the effects of nano particles when no magnetic field is applied. It shows that each increment of *φ* has a more prominent effect on the heat flux. The greater the φ, the higher is the heat flux. **Figure 10(b)** shows the same, with the application of a strong magnetic field. The behavior of heat flux is almost same as in **Figure 9(a)**. However, there is hardly any effect due to the magnetic field. Therefore, both **Figure 9** and **Figure 10** lead to same conclusion, that φ has the dominating effect on convection. This phenomenon can be explained by the nature of the thermal conductivity of nanofluid used in this work. For the base fluid and the nano particle considered, the thermal conductivity of the solid nano particles is significantly higher than that of the base fluid. Therefore, the nanoparticles carry significant amount of heat along with the base fluid. Thus, the overall heat transfer of the system is increased by adding more nanoparticles. Moreover, the nanoparticle has very low electrical conductivity and magnetic susceptibility, thus it is indifferent to the magnetic field applied. This finding has practical implications. It is possible to design efficient heat exchangers just by adding nano particles without worrying about magnetic interference from any source. However, it is possible that there is a cut-off limit for adding φ, beyond which the fluid will become too "thick" or too "heavy" for easy circulation, thus retarding heat transfer. This point can be a potential ground for future research.

7. Conclusion

Increasing φ reduced fluid velocity but enhanced heat transfer, while increasing Ha reduced fluid velocity and reduced heat transfer. The effect of Ha lost significance with increasing φ. For the values of Ra, Ha and φ considered in this work, it appears that φ is the most important factor in convection in a closed cavity. This finding has practical implications, with potential applications in heat exchanger design and operation.

Conflicts of Interest

The authors declare no conflicts of interest regarding the publication of this paper.

References

[1] NASA (2021) Welcome to the NASA's Guide to Hypersonic. https://www.grc.nasa.gov/WWW/BGH/bgh.html

[2] Mahjabin, S. (2019) Finite Element Analysis of MHD Free Convective Flow of Nano Fluid in a Square Cavity Containing a Heated Cone of Different Orientation. M. Phil. Thesis, Department of Mathematics, Bangladesh University of Engineering and Technology.

[3] Mahjabin, S. and Alim, M.A. (2018) Effect of Hartmann Number on Free Convective Flow of MHD Fluid in a Square Cavity with a Heated Cone of Different Orientation. *American Journal of Computational Mathematics*, **8**, 314-325. https://doi.org/10.4236/ajcm.2018.84025

[4] Mahjabin, S. and Alim, M.A. (2023) MHD Convection in a Square Cavity with a Heated Cone: Effects of Magnetic Field and Cone Orientation. *Journal of Bangladesh Academy of Sciences*, **47**, 127-137. https://doi.org/10.3329/jbas.v47i1.63983

[5] Chamkha, A.J., Jena, S.K. and Mahapatra, S.K. (2015) MHD Convection of Nanoflu-

ids: A Review. *Journal of Nanofluids*, **4**, 271-292. https://doi.org/10.1166/jon.2015.1166

[6] Choi, S.U.S. (1995) Enhancing Thermal Conductivity of Fluids with Nanoparticles. ASME Fluids Engineering Division, Vol. 231, 99-105.

[7] Yu, W. and Choi, S.U.S. (2003) The Role of Interfacial Layers in the Enhanced Thermal Conductivity of Nanofluids: A Renovated Maxwell Model. *Journal of Nanoparticle Research*, **5**, 167-171. https://doi.org/10.1023/a:1024438603801

[8] Khanafer, K., Vafai, K. and Lightstone, M. (2003) Buoyancy-Driven Heat Transfer Enhancement in a Two-Dimensional Enclosure Utilizing Nanofluids. *International Journal of Heat and Mass Transfer*, **46**, 3639-3653. https://doi.org/10.1016/s0017-9310(03)00156-x

[9] Jou, R. and Tzeng, S. (2006) Numerical Research of Nature Convective Heat Transfer Enhancement Filled with Nanofluids in Rectangular Enclosures. *International Communications in Heat and Mass Transfer*, **33**, 727-736. https://doi.org/10.1016/j.icheatmasstransfer.2006.02.016

[10] Tiwari, R.K. and Das, M.K. (2007) Heat Transfer Augmentation in a Two-Sided Lid-Driven Differentially Heated Square Cavity Utilizing Nanofluids. *International Journal of Heat and Mass Transfer*, **50**, 2002-2018. https://doi.org/10.1016/j.ijheatmasstransfer.2006.09.034

[11] Saidur, R., Leong, K.Y. and Mohammed, H.A. (2011) A Review on Applications and Challenges of Nanofluids. *Renewable and Sustainable Energy Reviews*, **15**, 1646-1668. https://doi.org/10.1016/j.rser.2010.11.035

[12] Qi, C., He, Y., Yan, S., Tian, F. and Hu, Y. (2013) Numerical Simulation of Natural Convection in a Square Enclosure Filled with Nanofluid Using the Two-Phase Lattice Boltzmann Method. *Nanoscale Research Letters*, **8**, Article No. 56. https://doi.org/10.1186/1556-276x-8-56

[13] Sheremet, M.A. and Pop, I. (2015) Natural Convection in a Wavy Porous Cavity with Sinusoidal Temperature Distributions on both Side Walls Filled with a Nanofluid: Buongiorno's Mathematical Model. *Journal of Heat Transfer*, **137**, Article ID: 072601. https://doi.org/10.1115/1.4029816

[14] Nemati, H., Farhadi, M., Sedighi, K., Ashorynejad, H.R. and Fattahi, E. (2012) Magnetic Field Effects on Natural Convection Flow of Nanofluid in a Rectangular Cavity Using the Lattice Boltzmann Model. *Scientia Iranica*, **19**, 303-310. https://doi.org/10.1016/j.scient.2012.02.016

[15] Ahmed, M. and Eslamian, M. (2015) Numerical Simulation of Natural Convection of a Nanofluid in an Inclined Heated Enclosure Using Two-Phase Lattice Boltzmann Method: Accurate Effects of Thermophoresis and Brownian Forces. *Nanoscale Research Letters*, **10**, Article No. 296. https://doi.org/10.1186/s11671-015-1006-0

[16] Ali, M.M., Alim, M.A. and Ahmed, S.S. (2018) Numerical Simulation of Hydromagnetic Natural Convection Flow in a Grooved Enclosure Filled with CuO-Water Nanofluid Considering Brownian Motion. *International Journal of Applied and Computational Mathematics*, **4**, Article No. 125. https://doi.org/10.1007/s40819-018-0563-1

[17] Mokaddes, A., Akhter, R. and Alim, A. (2020) MHD Natural Convection and Entropy Generation in a Grooved Enclosure Filled with Nanofluid Using Two Component Non Homogeneous Model. Springer Nature.

[18] Chamkha, A.J., Selimefendigil, F. and Oztop, H.F. (2020) Effects of a Rotating Cone on the Mixed Convection in a Double Lid-Driven 3D Porous Trapezoidal Nanofluid Filled Cavity under the Impact of Magnetic Field. *Nanomaterials*, **10**, Article No. 449.

https://doi.org/10.3390/nano10030449

[19] Alomari, M.A., Al-Farhany, K., Hashem, A.L., Al-Dawody, M.F., Redouane, F. and Olayemi, O.A. (2021) Numerical Study of MHD Natural Convection in Trapezoidal Enclosure Filled with (50%MgO-50%Ag/Water) Hybrid Nanofluid: Heated Sinusoidal from Below. *International Journal of Heat and Technology*, **39**, 1271-1279. https://doi.org/10.18280/ijht.390425

[20] Mondal, P., Mahapatra, T.R. and Parveen, R. (2021) Entropy Generation in Nanofluid Flow Due to Double Diffusive MHD Mixed Convection. *Heliyon*, **7**, e06143. https://doi.org/10.1016/j.heliyon.2021.e06143

[21] Sannad, M., Hussein, A.K., Abidi, A., Homod, R.Z., Biswal, U., Ali, B., *et al.* (2022) Numerical Study of MHD Natural Convection Inside a Cubical Cavity Loaded with Copper-Water Nanofluid by Using a Non-Homogeneous Dynamic Mathematical Model. *Mathematics*, **10**, Article No. 2072. https://doi.org/10.3390/math10122072

[22] Abdelhameed, T.N. (2022) Entropy Generation of MHD Flow of Sodium Alginate ($C_6H_9NAO_7$) Fluid in Thermal Engineering. *Scientific Reports*, **12**, Article No. 701. https://doi.org/10.1038/s41598-021-04655-0

[23] Banisi, S., Finch, J.A. and Laplante, A.R. (1993) Electrical Conductivity of Dispersions: A Review. *Minerals Engineering*, **6**, 369-385. https://doi.org/10.1016/0892-6875(93)90016-g

[24] Maxwell, J.C. (1892) Treatise of Electricity and Magnetism. 3rd Edition, Volume 1, Oxford University Press, 435-449.

[25] Pak, B.C. and Cho, Y.I. (1998) Hydrodynamic and Heat Transfer Study of Dispersed Fluids with Submicron Metallic Oxide Particles. *Experimental Heat Transfer*, **11**, 151-170. https://doi.org/10.1080/08916159808946559

[26] Dechaumphai, P. (1999) Finite Element Method in Engineering. 2nd Edition, Chulalongkorn University Press.

[27] Reddy, J.N. (1993) An Introduction to Finite Element Method. McGraw-Hill.

[28] Taylor, C. and Hood, P. (1973) A Numerical Solution of the Navier-Stokes Equations Using the Finite Element Technique. *Computers & Fluids*, **1**, 73-100. https://doi.org/10.1016/0045-7930(73)90027-3

Nomenclature, Greek Symbols and Subscripts

θ_{av}: average temperature
B_0: magnetic induction
C_p: Specific heat at constant pressure (J/kg K)
g: gravitational acceleration (m/s^2)
Gr: Grashof number
h: convective heat transfer coefficient (W/m^2 K)
Ha: Hartmann number
k: thermal conductivity of fluid (W/m K)
L: Height or base of trapezoidal cavity (m)
K: Thermal conductivity ratio fluid
N: Total number of nodes
Nu_{av}: Average Nusselt number
Nu_{local}: Local Nusselt number
P: non-dimensional pressure
p: pressure
Pr: Prandtl number
Ra: Rayleigh number
T: non-dimensional temperature
T_h: Temperature of hot bottom wall (k)
T_c: Temperature of cold top wall (k)
U: x component of dimensionless velocity
u: x component of velocity (m/s)
V: y-component of dimensionless velocity
v: y-component of velocity (m/s)
x, y: Cartesian coordinates
X, Y: dimensionless Cartesian coordinates
α: Thermal diffusivity (m^2/s)
β: Coefficient of thermal expansion (K^{-1})
ρ: Density of the fluid (kg/m^3)
$\Delta\theta$: Temperature difference
θ: Fluid temperature (dimensionless)
μ: Dynamic viscosity of the fluid (Pa s)
Ψ: Stream function
ν: Kinematic viscosity of the fluid (m^2/s)
σ: Fluid electrical conductivity ($\Omega^{-1}\cdot$m^{-1})
f: Base fluid
p: Nanoparticle (solid)